Applied and Environmental Microbiology, Oct. 2005, p. 5692–5701 Vol. 71, No. 10
0099-2240/05/$08.00+0 doi:10.1128/AEM.71.10.5692–5701.2005

Direct Labeling of Polyphosphate at the Ultrastructural Level in *Saccharomyces cerevisiae* by Using the Affinity of the Polyphosphate Binding Domain of *Escherichia coli* Exopolyphosphatase

Katsuharu Saito,[1]† Ryo Ohtomo,[1] Yukari Kuga-Uetake,[2] Toshihiro Aono,[3] and Masanori Saito[4]*

Department of Grassland Ecology, National Institute of Livestock and Grassland Science, 768 Senbonmatsu, Nishinasuno, Tochigi 329-2793, Japan[1]; Department of Food Production Science, Faculty of Agriculture, Shinshu University, 8304 Minami-minowa, Kami-ina, Nagano 399-4598, Japan[2]; Department of Biotechnology, Graduate School of Agricultural and Life Sciences, University of Tokyo, 1-1-1 Yayoi, Bunkyo-ku, Tokyo 113-8657, Japan[3]; and Department of Environmental Chemistry, National Institute for Agro-Environmental Sciences, 3-1-3 Kannondai, Tsukuba, Ibaraki 305-8604, Japan[4]

Received 13 December 2004/Accepted 29 April 2005

Inorganic polyphosphate (polyP) is a linear polymer of orthophosphate and has many biological functions in prokaryotic and eukaryotic organisms. To investigate polyP localization, we developed a novel technique using the affinity of the recombinant polyphosphate binding domain (PPBD) of *Escherichia coli* exopolyphosphatase to polyP. An epitope-tagged PPBD was expressed and purified from *E. coli*. Equilibrium binding assay of PPBD revealed its high affinity for long-chain polyP and its weak affinity for short-chain polyP and nucleic acids. To directly demonstrate polyP localization in *Saccharomyces cerevisiae* on resin sections prepared by rapid freezing and freeze-substitution, specimens were labeled with PPBD containing an epitope tag and then the epitope tag was detected by an indirect immunocytochemical method. A goat anti-mouse immunoglobulin G antibody conjugated with Alexa 488 for laser confocal microscopy or with colloidal gold for transmission electron microscopy was used. When the *S. cerevisiae* was cultured in yeast extract-peptone-dextrose medium (10 mM phosphate) for 10 h, polyP was distributed in a dispersed fashion in vacuoles in successfully cryofixed cells. A few polyP signals of the labeling were sometimes observed in cytosol around vacuoles with electron microscopy. Under our experimental conditions, polyP granules were not observed. Therefore, it remains unclear whether the method can detect the granule form. The method directly demonstrated the localization of polyP at the electron microscopic level for the first time and enabled the visualization of polyP localization with much higher specificity and resolution than with other conventional methods.

Inorganic polyphosphate (polyP) is a linear polymer of orthophosphate (P_i) connected by high-energy bonds. PolyP occurs in a wide range of organisms, including prokaryotes and eukaryotes. PolyP has various biological functions; for example, it acts as a P_i reservoir, as an alternative source of high-energy bonds, and as a buffer against alkaline conditions and metals (25). Furthermore, polyP also has regulatory functions such as competence for transformation (18), motility (36, 37), gene expression under stressed conditions (24, 35, 46), and protein degradation in amino acid starvation (28, 29) in prokaryotic organisms. The regulatory functions of polyP in eukaryotes are less clear, but some important facts are known. Recently, involvement of polyP in apoptosis (43) and enhancement of the mitogenic activities of acidic and basic fibroblast growth factors by polyP (45) have been suggested to occur in mammalian cells.

The presence of polyP in cells can be visualized by staining with toluidine blue O (TBO) or 4′,6-diamidino-2-phenylindole (DAPI). DAPI is usually used for DNA detection, because blue fluorescence is apparent when the stained tissues are viewed under UV light. However, DAPI-polyP fluoresces yellow at high concentrations when viewed under UV (48). These staining methods have often been used for detecting polyP-accumulating bacteria in activated sludge (38, 44, 47) and polyP accumulation in the hyphae of arbuscular mycorrhizal fungi (12). Also, subcellular localization of polyP has been investigated using both TBO and DAPI staining. Bacterial polyP is found in cellular inclusions known as metachromatic granules or volutin granules (26). In eukaryotic organisms, polyP has been shown to be localized in vacuoles (2), on the cell surfaces of yeasts (48), and in acidocalcisomes (30, 39, 41, 42), which are storage organelles for polyP and Ca^{2+} in protozoa and algae. TBO and DAPI are good probes for detecting cellular polyP easily, but it is sometimes difficult to determine the signals derived from polyP-bound probes, and the probes are not suitable for use in the ultrastructural analysis of polyP localization.

At the ultrastructural level, polyP appears as electron-dense regions, or the strong phosphorus signal of polyP is detected by electron microscopy coupled with energy-dispersive X-ray spectroscopy (EDXS) and electron energy loss spectroscopy (EELS). Phosphorus localization at the ultrastructural level has been investigated intensively by EDXS in ectomycorrhizal fungi, which are symbiotic organisms with plant roots that

* Corresponding author. Mailing address: Department of Environmental Chemistry, National Institute for Agro-Environmental Sciences, 3-1-3 Kannondai, Tsukuba, Ibaraki 305-8604, Japan. Phone and fax: 81 298 38 8300. E-mail: msaito@affrc.go.jp.

† Present address: CREST, Japan Science and Technology Corporation, Kawaguchi, Saitama 332-0012, Japan, and Graduate School of Science, University of Tokyo, Hongo, Bunkyo-ku, Tokyo 113-0033, Japan.

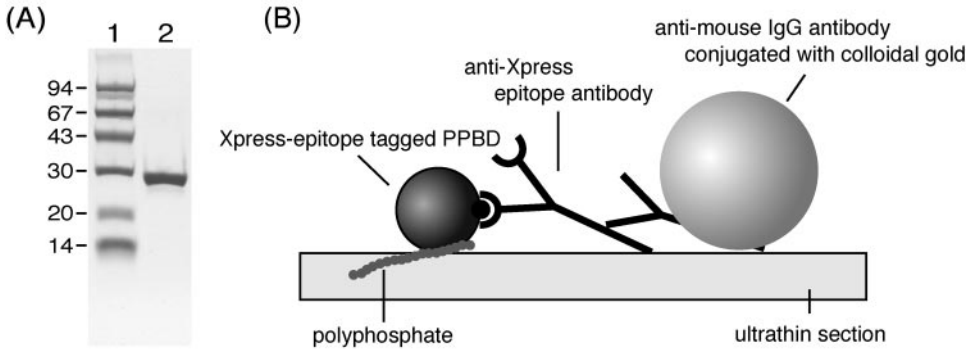

FIG. 1. (A) SDS-PAGE analysis of purified PPBD. Standards and samples were fractionated by 10% SDS-PAGE. Lane 1, size standards (in kilodaltons); lane 2, purified PPBD. (B) Schematic illustration of polyP labeling for transmission electron microscopic observation. polyP in ultrathin sections was treated with PPBD linked with an Xpress epitope tag. The epitope tag was detected by indirect immunogold labeling using anti-Xpress epitope antibody and secondary antibody conjugated with colloidal gold. For laser scanning confocal microscopic observation, the secondary antibody was conjugated with Alexa 488 instead of colloidal gold.

contribute to the improvement of plant nutrition (3, 4, 20). Formerly, on the basis of EDXS (6) and TBO staining (5), the polyP of ectomycorrhizal fungi was thought to be present as precipitated granules in vacuoles. However, polyP granules have been shown to be artifacts caused by ethanol dehydration following chemical fixation and by staining with cationic TBO (33). According to the results of EDXS analysis of freeze-substituted fungal hyphae, phosphorus in the vacuoles is not precipitated but is evenly dispersed, indicating that polyP is distributed in a soluble form in the vacuoles of living hyphae (7, 20, 33). However, polyP granules have been observed in nonfixed and air-dried algal cells (9) and in cryofixed and freeze-dried hyphae of ectomycorrhizal fungi (17). EELS is more advantageous for detecting light elements (e.g., phosphorus and nitrogen) and for spatial resolution than EDXS and has been used for P detection in polyP granules (13, 16, 22, 52). EELS can provide information on chemical bonding and the electronic states of compounds. However, it has not yet been used in such studies.

Here we developed a new technique to directly demonstrate polyP localization with high sensitivity and resolution by using the affinity of *Escherichia coli* exopolyphosphatase (PPX) for polyP. PPX is an enzyme that hydrolyzes the terminal phosphate bonds of polyP and consists of two domains, an N-terminal domain containing the PPX catalytic site and a C-terminal domain containing the polyP binding site (14, 15). In our procedure, polyP in thin sections of quick-frozen and freeze-substituted specimens was labeled with recombinant polyphosphate binding domain (PPBD) of PPX, containing an epitope tag at the N-terminal end, and then the epitope tag was detected by an indirect immunocytochemical method (Fig. 1B). We evaluated the specificity of binding of PPBD to polyP and demonstrated polyP localization in *Saccharomyces cerevisiae* by this PPBD affinity procedure.

MATERIALS AND METHODS

Strain and culture. *Saccharomyces cerevisiae* BY4741 (*MAT***a** *his3 leu2 met15 ura3*) was purchased from the American Type Culture Collection (Manassas, Va.). The yeast strain was grown at 30°C for 10 h in P_i-depleted yeast extract-peptone-dextrose (YPD) medium supplemented with either 0.2 mM (YPD-low P_i) or 10 mM (YPD-high P_i) potassium phosphate. P_i-depleted YPD was prepared as described previously (23, 40).

Purification of PPBD in PPX. Recombinant PPBD in PPX was prepared as described by Bolesch and Keasling (15), with the following modifications. The gene for the C-terminal PPBD of PPX (from glutamate 305) was amplified from the *E. coli* TOP10 f′ genome by PCR. Primers were 5′-CTGCAGAAATGGA AGGACGTTTCCGT-3′ and 5′-GAATTCCCCGCAAAGTATTAAGCGG-3′. The DNA amplified using these primers was first inserted into pGEM-T (Promega, Madison, Wisc.), creating pGEM-PPBD. The gene from pGEM-PPBD was then inserted into pTrc-HisB (Invitrogen, Carlsbad, Calif.), from the PstI (5′) to the EcoRI (3′) site, yielding pTrc-PPBD. *E. coli* TOP10 f′ harboring pTrc-PPBD was cultured in 50 ml SOB medium with 50 μg ml^{-1} ampicillin at 37°C. The culture was induced with 1 mM isopropylthio-β-D-galactoside (IPTG) at an A_{600} of 0.6. After incubation for 2 h, cells were harvested by centrifugation and resuspended in 10 ml binding buffer (10 mM HEPES-KOH [pH 7.6], 0.1 M NaCl, 5 mM $MgCl_2$, 0.05 mM EDTA, 2 mM β-mercaptoethanol, 10% glycerol). Cells were lysed six times using a sonicator with a 10-s pulse and centrifuged at 20,000 × *g* for 10 min at 4°C. The supernatant was filtered through a 0.2-μm cellulose acetate membrane filter (Advantec, Tokyo, Japan) and loaded on a 5-ml Ni^{2+}-charged HiTrap chelating HP column (Amersham, Piscataway, N.J.), preequilibrated with binding buffer, at a 2.5-ml min^{-1} flow rate, using a fast protein liquid chromatography system (Amersham). The column was washed with 50 ml washing buffer (10 mM HEPES-KOH [pH 7.6], 0.5 M NaCl, 5 mM $MgCl_2$, 0.05 mM EDTA, 2 mM β-mercaptoethanol, 10% glycerol). Recombinant protein was eluted with a linear imidazole gradient (0 to 0.5 M) in the binding buffer. The buffer was changed to 50 mM Tris-HCl (pH 9.0), using a PD-10 column (Amersham). An equal volume of glycerol was added to the purified protein, which was kept at −30°C for further use. Protein concentrations were measured by the Bio-Rad protein assay (Bio-Rad, Hercules, Calif.) with a bovine serum albumin (BSA) standard. Sodium dodecyl sulfate-polyacrylamide gel electrophoresis and staining with Coomassie brilliant blue R-250 were performed, using size standards from Amersham.

polyP binding assay for PPBD. [^{32}P]polyP was prepared as described by Kornberg and coworkers (1, 8), with the following modifications. One milliliter of reaction mixture contained 40 mM HEPES-KOH (pH 7.5), 50 mM $(NH_4)_2SO_4$, 4 mM $MgCl_2$, 4 mM creatine phosphate, about 30 U of creatine kinase, 1 mM ATP, 10 μl of [γ-^{32}P]ATP (3,000 Ci $mmol^{-1}$; Amersham), and 3 × 10^4 U of *E. coli* polyphosphate kinase (PPK) which was purified from PPK-overexpressing *E. coli*, as previously reported (1). After 4 h at 37°C, 100 μl of 0.5 M EDTA (pH 8.0) was added to stop the reaction. Size exclusion chromatography was performed to eliminate unincorporated ATP, using a PD-10 column (Amersham) with elution buffer of 1× Tris-EDTA (pH 8.0) with 100 mM NaCl. Eluted [^{32}P]polyP was precipitated by addition of a 0.75× volume of isopropanol. After incubation at room temperature for 20 min, [^{32}P]polyP was recovered by centrifugation at 20,000 × *g* for 10 min. The pellet was rinsed with 70% ethanol twice, dried by vacuum centrifugation, and resuspended in 100 μl of distilled water. The chain length of the [^{32}P]polyP was assumed to be close to 750 phosphate residues (8, 15). Unlabeled $polyP_{750}$ was also prepared as described above, but without the addition of [^{32}P]ATP. Short-chain [^{32}P]polyPs were prepared by limited hydrolysis of [^{32}P]$polyP_{750}$ in 10 mM HCl at 37°C for 30, 60, 90, 120, 180, and 240 min. The various short-chain polyP preparations were mixed together in a tube.

The equilibrium binding activity of PPBD to $polyP_{750}$ was measured by rapid filtration assay. PPBD was incubated in 50 μl of reaction mixture [25 mM Tris-HCl (pH 8.3), 137 mM NaCl, 2.7 mM KCl, 2 μg ml^{-1} (69 pmol ml^{-1}) PPBD, and the desired concentration of [^{32}P]$polyP_{750}$] at 0°C for 2 h. The reaction mixture was rapidly applied to a mixed cellulose membrane filter (0.45-μm pore size, 24-mm diameter; Millipore, Billerica, Mass.) prewetted with ice-cold washing buffer (25 mM Tris-HCl [pH 8.3], 137 mM NaCl, 2.7 mM KCl) on a vacuum filtration device. The filter was rinsed three times with 1 ml of ice-cold washing buffer and dried at room temperature. The bound polyP was quantified by liquid scintillation counting (LS6500; Beckman, Fullerton, Calif.). When 2,000 pmol of [^{32}P]$polyP_{750}$ was applied to the filter in the absence of PPBD and rinsed with the washing buffer, only 0.2% of the polyP was bound to the filter.

To characterize the reactivity of PPBD to short-chain polyP, the chain length of polyP unbound to the PPBD was analyzed by PAGE. The PPBD was incubated in 10 μl of reaction mixture [25 mM Tris-HCl (pH 8.3), 137 mM NaCl, 2.7 mM KCl, 40 μM of partially hydrolyzed [^{32}P]polyP in terms of P_i, and the desired concentration of PPBD] at 0°C for 2 h. The reaction mixture was rapidly applied to the membrane filter, and the filter was rinsed with 1 ml of ice-cold distilled water as described above. Bound polyP on the membrane filter was quantified by liquid scintillation counting. The reaction mixture that passed through the membrane filter was collected in a glass vial and concentrated by vacuum centrifugation. polyP analysis by PAGE was performed as described by Clark and Wood (19). Two microliters of the sample containing loading dye solution (1× Tris-borate-EDTA [TBE], 10% sucrose, and 0.025% bromophenol blue) was loaded on a 15% polyacrylamide gel (370 mm high, 280 mm wide, 0.35 mm thick) with 1× TBE buffer. The electrophoresis was run at 1,000 V until the bromophenol blue had migrated 14 cm. The gel was analyzed with a Molecular Imager system (Bio-Rad) with a Storage Phosphor Screen (Kodak, Rochester, N.Y.). Radioactive polyP size markers [$polyP_{39 \pm 2}$, $polyP_{56 \pm 3}$, $polyP_{88 \pm 5}$, and $polyP_{112 \pm 6}$] and a nonradioactive marker [$polyP_{58 \pm 10}$] were prepared by extracting polyP bands from the polyacrylamide gel of partially hydrolyzed polyP. [γ-^{32}P]ATP, partially hydrolyzed [^{32}P]polyP, and completely hydrolyzed [^{32}P]polyP as [^{32}P]orthophosphate were also used as size markers.

Competitive binding assay for PPBD. Inhibition of binding of [^{32}P]$polyP_{750}$ was assayed with the following unlabeled phosphate compounds: DNA (1-kb Plus DNA Ladder; Invitrogen), RNA (Yeast Total RNA; Ambion, Austin, Tex.), $polyP_{750}$, polyP type 75+ (Sigma), polyP type 35 (Sigma), polyP type 5 (Sigma), sodium tripolyphosphate (Sigma), sodium pyrophosphate (Sigma), and sodium phosphate (Wako, Osaka, Japan). PPBD was incubated in 50 μl of reaction mixture [25 mM Tris-HCl (pH 8.3), 137 mM NaCl, 2.7 mM KCl, 2 μg ml^{-1} (69 pmol ml^{-1}) PPBD, 40 μM [^{32}P]$polyP_{750}$ in terms of P_i, and the desired concentration of competitor] at 0°C for 2 h. The reaction mixture was rapidly transferred to the mixed cellulose membrane filter on a vacuum filtration device. The filter was rinsed three times with 1 ml of ice-cold washing buffer and dried at room temperature. The bound [^{32}P]$polyP_{750}$ was quantified by liquid scintillation counting. By using GraphPad Prism version 4.00 for Windows (GraphPad Software, San Diego, Calif.), the inhibition constant (K_i) was calculated from a model for competitive binding to two sites: $Y = SITE_1 + SITE_2 + NS$ (31), where Y is the total binding of [^{32}P]$polyP_{750}$, $SITE_1 = Hot \times B_{max1}/[Hot + K_{d1} \times (1 + Cold/K_{i1})]$, $SITE_2 = Hot \times B_{max2}/[Hot + K_{d2} \times (1 + Cold/K_{i2})]$, and NS is nonspecific binding. "Hot" is the concentration of [^{32}P]$polyP_{750}$ added to each tube, "Cold" is the concentration of unlabeled phosphate compound (competitor) added, B_{max1} and B_{max2} are the maximum bindings of the [^{32}P]$polyP_{750}$ for each site, K_{d1} and K_{d2} are the dissociation constants (K_d) of the [^{32}P]$polyP_{750}$ for each site, and K_{i1} and K_{i2} are K_is of the [^{32}P]$polyP_{750}$ for each site.

Quantification of polyP in *S. cerevisiae*. polyP was extracted from 2 ml of the yeast culture as described by Ogawa et al. (32). The polyP content was measured by *E. coli* PPK assay (8). polyP was assayed in a 20-μl reaction mixture [40 mM HEPES-KOH (pH 7.5), 40 mM $(NH_4)_2SO_4$, 4 mM $MgCl_2$, 40 μM ADP, 600 U PPK] incubated at 37°C for 40 min and then at 90°C for 2 min. The reaction mixture was diluted 1:100 with 100 mM Tris-HCl (pH 8.0) containing 4 mM EDTA, of which 20 μl was added to the same volume of CLSII reaction mixture (Roche Diagnostics, Basel, Switzerland). Chemiluminescence was measured with a Luminescencer PSN (Atto, Tokyo, Japan) as the total luminescence count in 10 s. The concentration of polyP is given in terms of P_i residues.

PAGE of *S. cerevisiae* polyP. Five milliliters of culture solution was centrifuged and suspended in 400 μl acetone. The cells were disrupted with a bead beater (BioSpec Products, Bartlesville, Okla.) for three times 10 s each at 5,000 rpm using 200 mg of zirconia beads (0.5 mm in diameter). Acetone was evaporated by vacuum centrifugation. The pellet was suspended in 400 μl distilled water, and the suspension was extracted with phenol-chloroform followed by chloroform extraction. The aqueous phase was used for polyP analysis by PAGE. Two microliters of the sample containing the loading dye solution was loaded on 15% and 8% polyacrylamide gels with 1× TBE buffer. The electrophoresis was run at 1,000 V until the bromophenol blue had migrated 14 cm. The gel was soaked in 10% methanol–10% acetate for 10 min, stained with 0.5% TBO–25% methanol–5% acetate–5% glycerol for 10 min, and then destained in 25% methanol–5% acetate–5% glycerol.

Quick freezing and freeze-substitution. One milliliter of yeast culture was centrifuged, and a portion of the precipitate was transferred onto a Formvar membrane spread around a copper loop with a handle (3 mm in diameter; 15 mm long). The loop was further covered by a Formvar membrane, and excess water on the loop was removed with a piece of filter paper. The loop was then quickly frozen by plunging it into liquid propane cooled with liquid nitrogen. Frozen samples were transferred to a substitution medium of 100% dry acetone containing Molecular Sieves 4A 1/16 (Wako). The samples were substituted at −80°C for 3 days and warmed at −20°C for 2 h, 4°C for 2 h, and room temperature for 2 h. The samples were immersed twice in 100% dry acetone for 10 min before being infiltrated with Spurr's resin mixed with acetone (25% resin, 50% resin, and 75% resin; 12 h for each step) and then with pure resin for 2 days (resin was replaced once at 24 h). The samples were polymerized at 70°C overnight. Embedded materials were sectioned with an ultramicrotome (Leica, Bannockburn, Ill.). Sections about 70 nm thick for electron microscopy were cut with a diamond knife and picked up on 200-mesh nickel grids. Semithin sections were cut with glass knives to 300-nm thickness and collected on aminosilane-coated glass slides (Matsunami, Osaka, Japan).

polyP detection using PPBD affinity labeling with LSCM. Sections were immersed for 10 min at room temperature in methanol containing 10% H_2O_2. The sections were washed with distilled water. Specimens were blocked for 10 min at room temperature with Tris-buffered saline (pH 8.3) (TBS) containing 1% BSA. Samples were first incubated at room temperature overnight in a mixture of 20 μg ml^{-1} PPBD, 10 μg ml^{-1} mouse anti-Xpress epitope antibody (Invitrogen), TBS, and 1% BSA. Samples were washed with TBS containing 0.05% Triton X-100 with or without 0.2 M imidazole and then washed with TBS. Semithin sections were incubated for 2 h at room temperature with a goat anti-mouse immunoglobulin G (IgG) antibody conjugated with Alexa 488 (Molecular Probes, Eugene, Oreg.) diluted 1:5,000 in TBS containing 1% BSA. Samples were sequentially washed with TBS containing 0.05% Triton X-100, TBS, and distilled water. Negative controls were prepared by incubating sections without PPBD, mouse anti-Xpress antibody, or labeled goat anti-mouse IgG antibody or without both PPBD and mouse anti-Xpress antibody. Another negative control was prepared by incubating sections with an excessive amount of competitor (100 mM tripolyphosphate) during the first reaction. Fluorescence microscopy was performed by laser scanning confocal microscopy (LSCM) (LSM510; Carl Zeiss, Jena, Germany). The fluorescence of Alexa 488 was excited by using a 488-nm-wavelength argon laser, and the fluorescence emitted was detected with a 505- to 550-nm band-pass filter. Autofluorescence was detected with a 580-nm long-pass filter, using a 546-nm He-Ne laser for excitation. Image analysis was performed with LSM510 software version 2.5 (Carl Zeiss).

PolyP detection using PPBD affinity labeling with TEM. Ultrathin sections were immersed in the H_2O_2-methanol, blocked in TBS containing BSA, and incubated in a mixture of PPBD, mouse anti-Xpress epitope antibody, TBS, and BSA as described above for LSCM. The ultrathin sections were incubated for 2 h at room temperature with a goat anti-mouse IgG antibody conjugated with 10-nm colloidal gold (BBInternational, Cardiff, United Kingdom) diluted 1:100 in TBS containing 1% BSA. After labeling, the ultrathin sections were stained with uranyl acetate followed by lead citrate and observed by transmission electron microscopy (TEM) (H-7100; Hitachi, Tokyo, Japan) at an accelerating voltage of 75 kV.

RESULTS

Purification of PPBD. To obtain PPBD for polyP labeling, we constructed an expression vector in which the PPBD sequence was linked to sequences of the Xpress epitope and His_6. The Xpress epitope was used to detect PPBD localization by immunocytochemistry, and the His_6 was used for purification by affinity chromatography. The PPBD expressed in *E. coli* was purified using an Ni^{2+}-charged affinity column. To elute PPBD from the affinity column, approximately 0.2 M imidazole was required. The eluted PPBD was purified as a single band

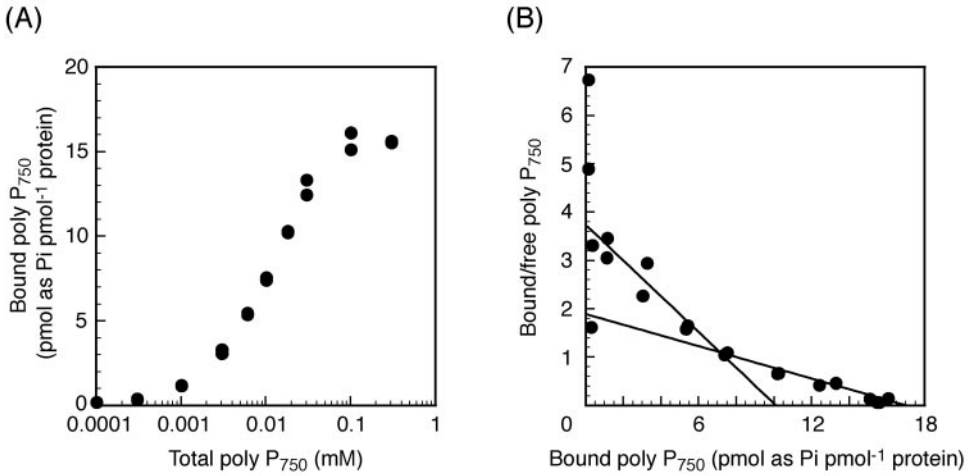

FIG. 2. Equilibrium binding of polyP$_{750}$ to purified PPBD (A) and a Scatchard plot (B). The Scatchard transform of equilibrium binding yielded two binding sites.

by SDS-PAGE analysis, and its size was approximately 29 kDa (Fig. 1A).

Binding assay of PPBD. Equilibrium binding of polyP$_{750}$ to PPBD is shown in Fig. 2A. A Scatchard transform of the equilibrium binding yielded two binding sites (Fig. 2B), a high-affinity site (K_{d1} = 2.0 μM as P_i) and a lower-affinity site (K_{d2} = 12.0 μM as P_i).

An experiment on equilibrium binding of partially hydrolyzed polyP to PPBD was carried out to characterize the PPBD affinity for short-chain polyP. From PAGE analysis of unbound polyP, the distribution of the unbound polyP chain length was shown to shift to short chain as the PPBD concentration increased (Fig. 3A). When 40 μM of partially hydrolyzed polyP was incubated with 3.4×10^4 pmol ml^{-1} PPBD in which polyP binding sites were almost saturated (Fig. 3B), PPBD bound to most polyP longer than 35 residues. PPBD at concentrations of 6.9×10^3 and 1.4×10^3 pmol ml^{-1} bound to polyP of >50 and >80 residues, respectively. PPBD bound to only a small amount of short polyP (<30 residues), even when a high concentration of PPBD was used.

To determine the affinity of PPBD for short-chain polyP and other high-molecular-weight phosphate compounds, we compared the inhibition of polyP$_{750}$ binding among the phosphate compounds. Some polyP reagents obtained from Sigma are known to be mixtures of a wide range of polyPs (19, 55). polyP type 75+ consisted mainly of polyP longer than 40 residues (Fig. 4C). polyP type 35 and type 5 consisted of polyP shorter than 120 to 150 and 20 residues, respectively (Fig. 4C). The curves in Fig. 4 and K_i values in Table 1 were calculated by nonlinear regression, using a model for competitive binding to two sites. As the polyP chain length of competitors became shorter, the K_i value of [^{32}P]polyP$_{750}$ binding increased (Fig. 4A and Table 1). Orthophosphate hardly inhibited [^{32}P]polyP$_{750}$ binding to PPBD. The affinities of PPBD for polyP type 75+, polyP type 35, polyP type 5, tripolyphosphate, pyrophosphate, and orthophosphate were about 7 to 8, 35, 260, 80, 230, and 3,200 times lower, respectively, than that for polyP$_{750}$. The K_i value by DNA was almost equal to that by polyP type 35 when the concentration of nucleic acid was expressed as molar values in terms of P_i (Fig. 4B and Table 1). The K_i value by RNA was between those by polyP type 35 and tripolyphosphate. When the nucleic acid concentration was expressed in milligrams per milliliter, the K_i value by DNA was between those for tripolyphosphate and pyrophosphate, and the K_i value by RNA was nearly equal to that by pyrophosphate (data not shown).

polyP content and length in *S. cerevisiae*. The polyP content of *S. cerevisiae* incubated in YPD-high P_i for 10 h was 2,383 nmol as P_i mg^{-1} protein, which was 340 times higher than the polyP content (7 nmol as P_i mg^{-1} protein) of *S. cerevisiae* incubated in YPD-low P_i. The chain length of polyP extracted from *S. cerevisiae* in YPD-high P_i was less than 150 residues in PAGE analysis (Fig. 5). Longer chains of polyP were detected in 8% PAGE analysis (Fig. 5, lane 4), but their amounts were very small.

polyP labeling using PPBD affinity. (i) LSCM. polyP localization was visualized by fluorescence-based polyP labeling using PPBD affinity (Fig. 6). Initially, sections were sequentially incubated in PPBD solution, anti-Xpress antibody solution, and anti-mouse IgG antibody solution. This procedure gave a highly fluorescent background. This problem was overcome by sequentially incubating the sections in a solution of PPBD–anti-Xpress antibody complex and then anti-mouse IgG antibody solution. Signals from labeled polyP were exhibited as green fluorescence of Alexa 488, but some green fluorescence was derived from autofluorescence of collapsed cells. The polyP signal could be discriminated from autofluorescence by overlaying images excited by an He-Ne laser (wavelength, 546 nm), because the autofluorescence had a broad emission spectrum. Intense labeling was observed in the vacuoles (Fig. 6a and b). The distribution in vacuoles was dispersed (Fig. 6b). Many cells incubated in YPD-high P_i contained polyP, but not all cells did (Fig. 6a). In YPD-low P_i, few cells showed the polyP signal (Fig. 6c). No polyP signal was detected in the negative controls, in which PPBD and/or antibody had been removed from the reaction mixture (Fig. 6d, e, f, and g) or in which the polyP binding site of PPBD had been saturated with a high concentration of tripolyphosphate (Fig. 6h).

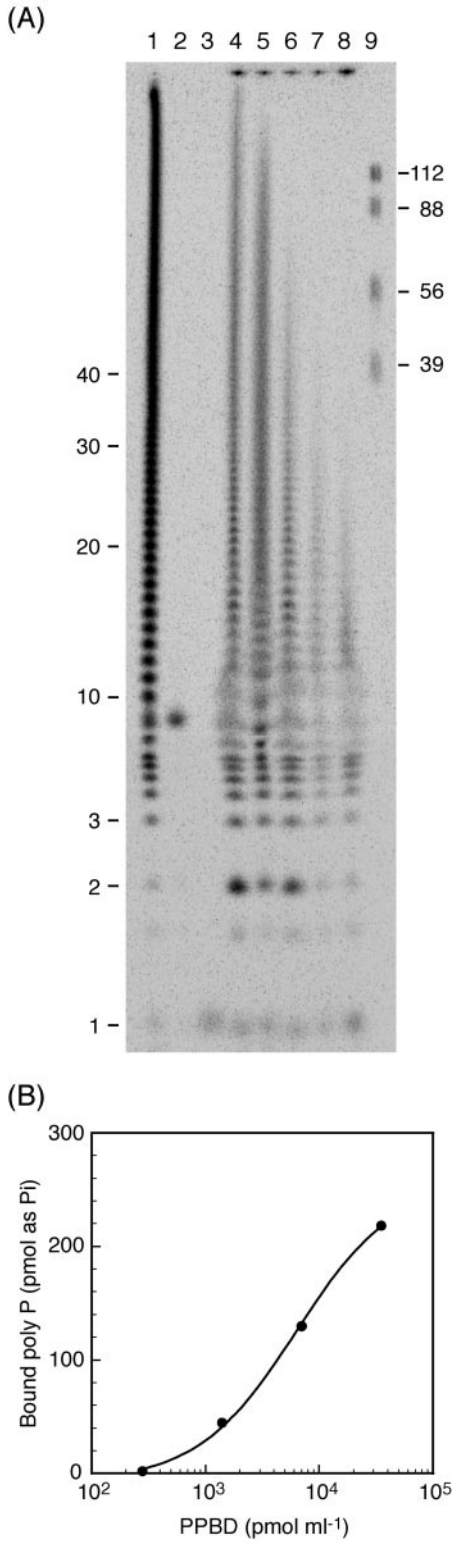

FIG. 3. Equilibrium binding of partially hydrolyzed polyP to PPBD. (A) PAGE (15%) analysis of polyP unbound to PPBD. Lane 1, partially hydrolyzed polyP as size ladder; lane 2, ATP; lane 3, orthophosphate; lanes 4 to 8, polyP unbound to 0, 2.8×10^2, 1.4×10^3, 6.9×10^3, and 3.4×10^4 pmol ml^{-1} PPBD, respectively; lane 9, polyP size markers. Numbers on both sides indicate chain lengths of polyP. Bands between P_1 and P_2 are hexametaphosphate. (B) Equilibrium binding of partially hydrolyzed polyP to PPBD.

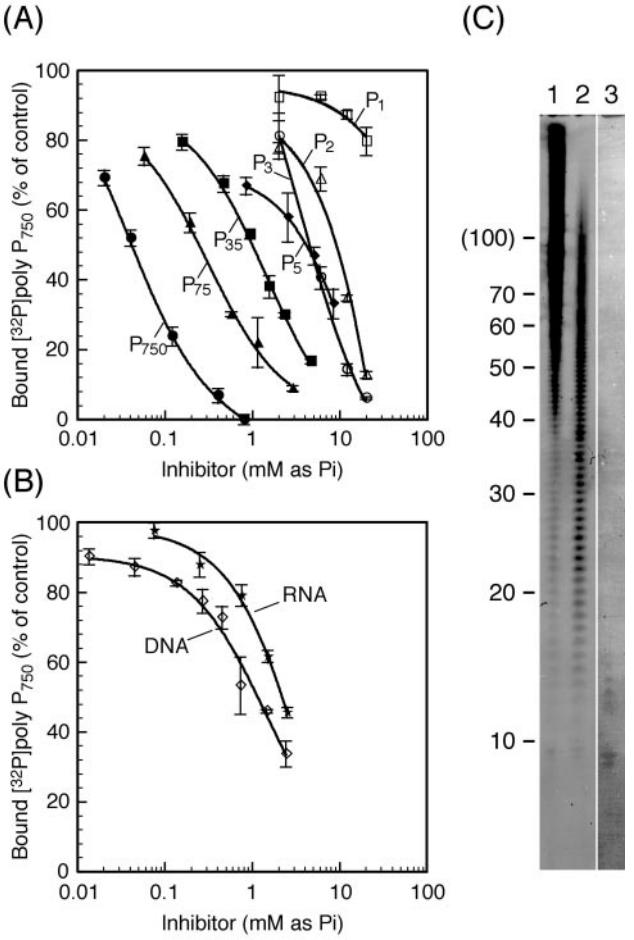

FIG. 4. Inhibition of [^{32}P]polyP_{750} binding to PPBD by unlabeled phosphate compounds. (A) Inhibition by various types of polyP. P_{750}, unlabeled polyP_{750}; P_{75}, polyP type 75+; P_{35}, polyP type 35; P_5, polyP type 5; P_3, tripolyphosphate; P_2, pyrophosphate; P_1, orthophosphate. (B) Inhibition by DNA and RNA. Concentrations are expressed in terms of P_i. (C) Size distribution of polyP type 75+ (lane 1), type 35 (lane 2), and type 5 (lane 3), analyzed by PAGE (15%). polyP was stained with toluidine blue O. Numbers on the left indicate chain lengths of polyP, which were determined from size ladders of partially hydrolyzed [^{32}P]polyP. The value in parentheses was estimated from reference (19). Error bars indicate standard deviations.

(ii) TEM. An ultrastructural method of polyP detection was developed using TEM. With this method, colloidal gold instead of the fluorescent probe was conjugated to the secondary antibody. When the samples were fixed, osmium tetroxide was not used because the reagent reduced the polyP signal intensity (data not shown). Most signals were observed in the vacuoles of *S. cerevisiae* in YPD-high P_i (Fig. 7a, b, c, and d). The density of colloidal gold in vacuoles was different among cells, even in the same section: dense (Fig. 7a) to sparse (Fig. 7b) to no signal (data not shown). polyP signals were found all over the vacuole and seemed to be located on flocculent material within the vacuole. The polyP distribution was not completely homogenous within individual vacuoles; some regions were dense, and some were sparse (Fig. 7c). In most cells signals were barely observed in the nuclei and mitochondria (Fig. 7a and c), although some signals were often observed around the vacu-

TABLE 1. Affinities of PPBD for phosphate compounds[a]

Competitor	μM as P_i	
	K_{i1}	K_{i2}
$polyP_{750}$	2	10
polyP type 75+	13	83
polyP type 35	70	339
polyP type 5	533	2,588
Tripolyphosphate	167	807
Pyrophosphate	471	2,280
Orthophosphate	6,592	31,915
DNA	67	324
RNA	131	635

[a] Inhibition constants (K_i) were determined from displacement of [^{32}P]$polyP_{750}$ binding to polyP binding sites on PPBD.

oles (Fig. 7c and d). However, we did not determine whether the polyP signals were in or on a certain organelle or in the cytoplasm. This is because osmium tetroxide was not used for fixation, and there was low contrast for membrane structure. Intense signals were not observed in the cells incubated in YPD-low P_i, whereas a few signals were occasionally found around the vacuoles (data not shown). There was no polyP signal in the negative controls, where sections of *S. cerevisiae* (YPD-high P_i) were incubated in reaction mixture without PPBD (Fig. 7e), without mouse anti-Xpress antibody (Fig. 7e), without both PPBD and mouse anti-Xpress antibody (data not shown), or without goat anti-mouse IgG antibody conjugated with 10-nm colloidal gold (data not shown). There was also no polyP signal when the polyP binding site of PPBD was masked with a high concentration of tripolyphosphate. To check for nonspecific binding of PPBD by the His_6 tag, sections were washed with an imidazole-containing buffer after PPBD incubation. The signal distribution was not different in treatments with and without imidazole, indicating that the His_6 tag did not affect the polyP labeling.

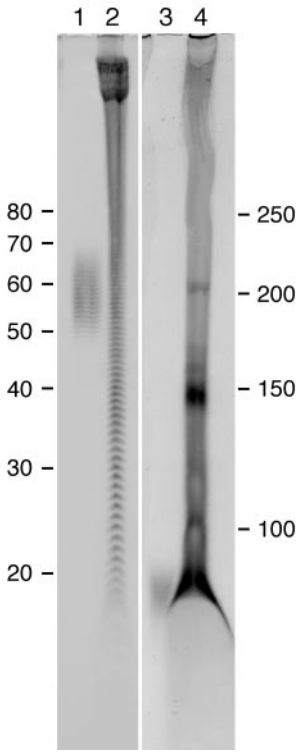

FIG. 5. PAGE analysis of *Saccharomyces cerevisiae* polyP. polyP extracted from *S. cerevisiae* cultured in YPD containing 10 mM phosphate (YPD-high P_i) (lanes 2 and 4) was fractionated by 15% (lanes 1 and 2) and 8% (lanes 3 and 4) PAGE. polyP size markers (lanes 1 and 3) are $polyP_{58 \pm 10}$. Numbers on the left indicate chain lengths of polyP, which were determined from size markers. Chain lengths indicated on the right were estimated from reference (19). Some RNA bands were recognized near the top in lane 2 and near residues 150 and 200 of polyP in lane 4.

DISCUSSION

We developed a novel procedure to specifically detect polyP with high spatial resolution at the ultrastructural level. EDXS and EELS detect phosphorus elements, but no direct detection method for polyP at the ultrastructural level has been available. A novel aspect of the procedure was to use PPBD linked with an epitope tag. Immunocytochemical methods are usually used to investigate the localization of biological molecules. However, it seemed difficult to use immunological techniques in the analysis of polyP localization because of the difficulty in raising specific antibodies against polyP. We examined the use of PPX, which exhibits specific binding to polyP in the evolutionary process. One of the methods that uses the specific affinity of an enzyme to its substrate is the enzyme-gold procedure, where an enzyme directly bound to colloidal gold is applied to sections and then the substrate is visualized as signals of colloidal gold (11). Initially, we tried an enzyme-gold procedure in which purified PPX bound to colloidal gold was used. The PPX-gold complex exhibited little binding to polyP (data not shown). This may have been because the polyP binding site of the PPX was masked by the colloidal gold. Next, we developed a method in which an epitope tag on PPBD bound to polyP was detected immunocytochemically.

Affinity assays of PPBD and control experiments with polyP labeling showed that fluorescent and colloidal gold signals by the polyP labeling specifically represented polyP localization. Cellular polyP consists of polymers of various chain length. PPX has been reported to have polyP binding sites in its C-terminal domain (15), but their affinities to various lengths of polyP or other phosphate compounds, including nucleic acids, were unknown. The competitive binding assay (Fig. 4B and Table 1) indicated that the PPBD of PPX binds strongly to long-chain polyP but is not able to bind short-chain polyP unless the polyP is at a high concentration. Unexpectedly, polyP type 5 showed lower affinity than did tripolyphosphate and pyrophosphate (Table 1). This could be because the polyP type 5 contains orthophosphate, pyrophosphate, and tripolyphosphate other than $polyP_4$ to $polyP_{20}$. From the binding assay, we found that polyP labeling using PPBD was suitable for detecting long-chain polyP. However, it may be difficult to detect short-chain polyP because of the low affinity. It is also possible that short-chain polyP was eluted from the sections during labeling. The affinity of the PPBD for nucleic acid was not as high as that for long-chain polyP. The low affinity for nucleic acid was also confirmed from polyP labeling of yeast, in

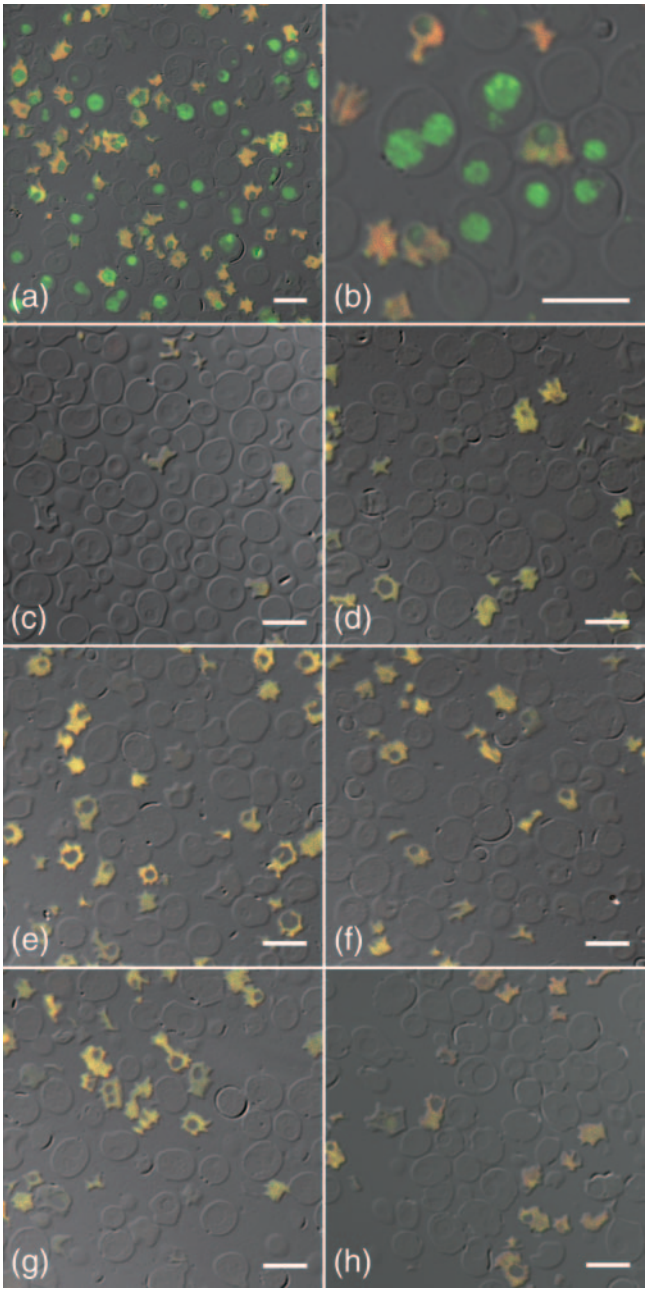

FIG. 6. Laser scanning confocal images of polyP distribution. PolyP was labeled with PPBD–anti-Xpress antibody complex followed by anti-mouse IgG antibody conjugated with Alexa 488 (a to c) or various controls (d to h). Fluorescent images of Alexa 488 and autofluorescent images were superimposed with pseudo-differential interference contrast images. Fluorescence of Alexa 488 appears green. Some green fluorescence was derived from autofluorescence of collapsed cells. The polyP signal was discriminated from the autofluorescence (yellow to red) by overlaying images excited by an He-Ne laser (wavelength, 546 nm), because the autofluorescence had a broad emission spectrum. (a) Sections of *Saccharomyces cerevisiae* incubated in YPD containing 10 mM phosphate (YPD-high P_i). Intense polyP signals were detected in vacuoles of *S. cerevisiae* cells. (b) Highly magnified image of *S. cerevisiae* incubated in YPD-high P_i. polyP is distributed in a dispersed manner in the vacuoles. (c) Sections of *S. cerevisiae* incubated in YPD containing 0.2 mM phosphate (YPD-low P_i). Few polyP signals were detected in the cells. (d to h) Negative controls of polyP labeling using PPBD affinity. Sections of *S. cerevisiae* (YPD-high P_i) were incubated in reaction mixtures without PPBD (d), without mouse anti-Xpress antibody (e), without both PPBD and mouse anti-Xpress antibody (f), and without goat anti-mouse IgG antibody conjugated with Alexa 488 (g) or in a mixture of PPBD–anti-Xpress antibody complex to which had been added 100 mM tripolyphosphate (h). Bars, 5.0 μm.

which few colloidal gold particles were observed on DNA in the nuclei and mitochondria. In a preliminary experiment with polyP labeling using PPBD, the addition of osmium tetroxide to samples for ultrastructural analysis led to a reduction in the polyP signal. This would be because the osmium forms complexes with polyP and then the amount of free polyP available to bind to the PPBD decreases. Another point of note is that polyP signals gradually decrease with time after the sections are made. This may be because polyP in sections is degraded or oxidized, so that the PPBD cannot then bind to these compounds.

The size of yeast polyP was less than about 150 residues when the yeast was incubated in P_i-rich medium (Fig. 5). This size distribution is similar to that of polyP type 35. Therefore, the affinity of PPBD for the yeast polyP would be similar to that for polyP 35 in the phosphate compounds tested. Most polyP was distributed in vacuoles (Fig. 6 and 7). This result was consistent with a study of subcellular fractionation (53), in which the vacuole fraction was shown to contain large amounts of polyP. However, Trilisenko et al. (51) reported that vacuolar polyP of yeast accounted for only about 15% of the total polyP, and they suggested that the vacuolar polyP content is dependent on the strain, culture conditions, developmental stage, or method of vacuole isolation. Orlovich and Ashford (33) demonstrated that phosphorus observed by EDXS was evenly dispersed in vacuoles when *Pisolithus tinctorius* hyphae were fixed by cryofixation and freeze-substitution, although the fungal vacuoles were treated by conventional chemical fixation and contained precipitated phosphorus-rich granules. They suggested that the precipitated granules were artifacts caused by dehydration during chemical fixation and that vacuolar polyP exists in a soluble form in living cells. On the other hand, Bücking and Heyser (17) observed granules in the vacuoles of living hyphae with light microscopy and showed by EDXS analysis of cryofixed and freeze-dried samples that there were phosphorus-containing granules in the vacuoles. In our observation of yeast cells, vacuolar polyP was dispersed, not precipitated, when the cells were fixed by quick freezing and freeze-substitution. More detailed observation revealed that the polyP distribution in the vacuoles was somewhat heterogeneous (Fig. 7c). Under our experimental conditions, we did not observe electron-dense structures, such as polyP granules, in the vacuoles or cytoplasm. Thus, we could not examine whether the polyP detection method is possible for the granule form. PolyP granules have been isolated from yeast cells under polyP overcompensation conditions in which phosphate-starved yeast cells are incubated in phosphate-rich medium (21). Therefore, there is a possibility that polyP in yeast cells could be in two forms, soluble or precipitated, depending on the cultural conditions, on the physiological state of the cells, and/or on a process of polyP accumulation. Further research on the form and localization of polyP in yeast cells in terms of cultural conditions and physiological states is necessary.

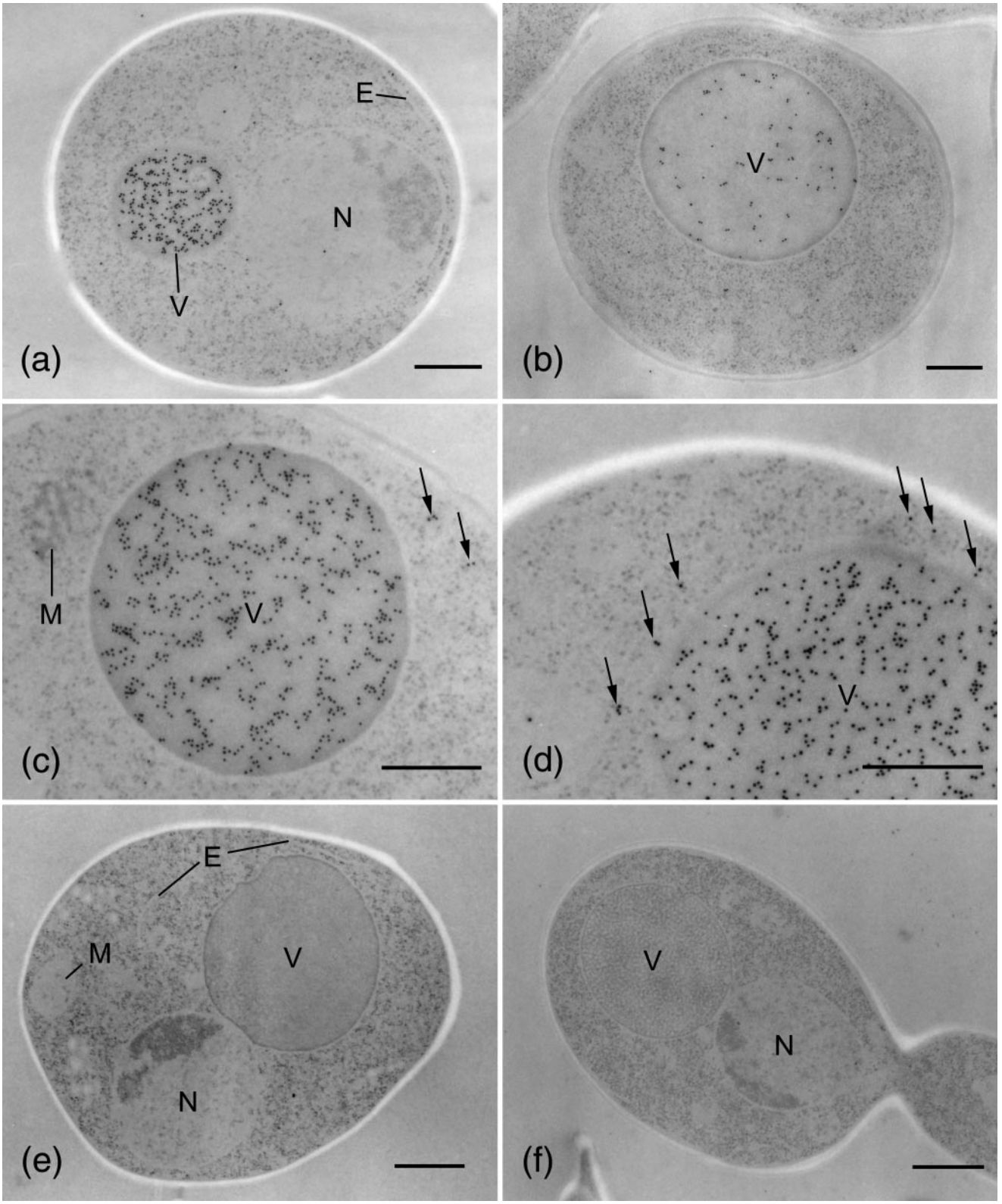

FIG. 7. Transmission electron micrographs of polyP distribution. PolyP was labeled with PPBD–anti-Xpress antibody complex followed by anti-mouse IgG antibody conjugated with 10-nm colloidal gold. Sections of *Saccharomyces cerevisiae* were incubated in YPD-high P_i. (a) PolyP signal distribution in an *S. cerevisiae* cell. Intense PolyP signals were found in the vacuoles. In the nucleus, few signals were detected. (b) polyP signals were found in the vacuole, but the signal density was not very high in this cell. (c) Highly magnified image of a yeast vacuole. Signals were found all over the vacuole, but their distribution was not completely homogenous. Some polyP signals (arrows) were detected around the vacuole. (d) PolyP signals (arrows) around the vacuole. (e and f) Negative controls of polyP labeling using PPBD affinity. Sections of *S. cerevisiae* were incubated in reaction mixtures without PPBD (e) and without mouse anti-Xpress antibody (f). E, endoplasmic reticulum; M, mitochondria; N, nucleus; V, vacuole. Bars, 500 nm.

PolyP was also observed at low density around the vacuoles (Fig. 7c and d). It was not clear whether the polyP was in the cytosol, endoplasmic reticulum, or other organelles, because osmium tetroxide was omitted during the fixation, thus reducing the image contrast. However, strong evidence for the presence of polyP in nonvacuolar compartments has been provided by subcellular fractionation and cytological staining. Trilisenko et al. (51) showed that the cytosol fraction of yeast contained much polyP. Other circumstantial evidence of cytosolic polyP is the fact that yeast exopolyphosphatase (PPX1) has been isolated from the cytosol fraction (56, 57), implying that polyP, a substrate of PPX1, exists in the cytosol. In our study, polyP signals were barely detectable in the nuclei and mitochondria. However, several studies have showed that polyP is detected in the nuclei of *Neurospora crassa*, *Endomyces magnusii* (26), and mammalian cells (27) by cell fractionation and in yeast mitochondria by ^{31}P nuclear magnetic resonance (10). The amounts of polyP in the nuclei and mitochondria are not very large compared with the amounts of vacuolar polyP. PolyP in yeast mitochondria consists of short chains of less than 15 residues (34). Because of the small amount of polyP present or its short chain length, our procedure using PPBD might not have detected polyP signals in the mitochondria. Many researchers have described polyP in the cell periphery, the cell envelope, or the cell wall in yeasts (48–50, 54) and *E. magnusii* (26). However, we could not detect polyP signals in such structures in *S. cerevisiae*. The presence of polyP in the structures seems to depend on the fungal species and incubation conditions. Tijssen et al. (48) showed that polyP on the cell envelope was detected in *Saccharomyces fragilis* by DAPI staining but not in *S. cerevisiae*. However, *S. cerevisiae* can accumulate polyP on the outer membrane when the cells are incubated in P_i-rich medium after phosphate starvation (54).

In summary, we demonstrated a new technique, based on enzymatic affinity and immunocytochemistry, for the analysis of polyP localization. We also showed that most of the long-chain polyP detected by our procedure was distributed in the yeast vacuoles in a dispersed manner, and a much smaller amount of polyP was localized around the vacuoles. This polyP detection method will provide new insight into the biology of polyP. Furthermore, we expect that this kind of method will be applicable to the detection of other biological macromolecules.

ACKNOWLEDGMENTS

We thank Arthur Kornberg and his coworkers for their kind distribution of the PPK-overexpressing *E. coli* strain. We thank R. Larry Peterson for his valuable suggestions and critical reading of the manuscript.

This work was supported in part by the Promotion of Basic Research Activities for Innovative Biosciences (PROBRAIN) of the Bio-oriented Technology Research Advancement Institution, Japan. K.S. was awarded an Organization for Economic Co-operation and Development (OECD) fellowship under the Co-operative Research Programme: Biological Resource Management for Sustainable Agricultural Systems.

REFERENCES

1. **Ahn, K., and A. Kornberg.** 1990. Polyphosphate kinase from *Escherichia coli*. purification and demonstration of a phosphoenzyme intermediate. J. Biol. Chem. **265:**11734–11739.
2. **Allan, R. A., and J. J. Miller.** 1980. Influence of *S*-adenosylmethionine on DAPI-induced fluorescence of polyphosphate in the yeast vacuole. Can. J. Microbiol. **26:**912–920.
3. **Ashford, A. E.** 1998. Dynamic pleiomorphic vacuole systems: are they endosomes and transport compartments in fungal hyphae? Adv. Bot. Res. **28:** 119–159.
4. **Ashford, A. E., L. Cole, and G. J. Hyde.** 2001. Motile tubular vacuole systems, p. 243–265. *In* R. J. Howard and N. A. R. Gow (ed.), The Mycota: biology of the fungal cell, vol. VIII. Springer-Verlag, Berlin, Germany.
5. **Ashford, A. E., M. Ling-Lee, and G. A. Chilvers.** 1975. Polyphosphate in eucalypt mycorrhizas: a cytochemical demonstration. New Phytol. **74:**447–453.
6. **Ashford, A. E., R. L. Peterson, D. Dwarte, and G. A. Chilvers.** 1986. Polyphosphate granules in eucalypt mycorrhizas: determination by energy dispersive X-ray microanalysis. Can. J. Bot. **64:**677–687.
7. **Ashford, A. E., P. A. Vesk, D. A. Orlovich, A.-L. Markovina, and W. G. Allaway.** 1999. Dispersed polyphosphate in fungal vacuoles in *Eucalyptus pilularis*/*Pisolithus tinctorius* ectomycorrhizas. Fungal Genet. Biol. **28:**21–33.
8. **Ault-Riché, D., C. D. Fraley, C-M. Tzeng, and A. Kornberg.** 1998. Novel assay reveals multiple pathways regulating stress-induced accumulations of inorganic polyphosphate in *Escherichia coli*. J. Bacteriol. **180:**1841–1847.
9. **Baxter, M., and T. E. Jensen.** 1986. Cell volume occupied by polyphosphate bodies during the polyphosphate overplus phenomenon in *Plectonema boryanum*. Cytobios **45:**147–160.
10. **Beauvoit, B., M. Rigoulet, B. Guerin, and P. Canioni.** 1989. Polyphosphates as a source of high energy phosphates in yeast mitochondria: a ^{31}P NMR study. FEBS Lett. **252:**17–21.
11. **Bendayan, M.** 1989. Colloidal gold: principles, methods, and applications, vol. 2, p. 117–147. Academic Press, San Diego, Calif.
12. **Boddington, C. L., and J. C. Dodd.** 1999. Evidence that differences in phosphate metabolism in mycorrhizas formed by species of *Glomus* and *Gigaspora* might be related to their life-cycle strategies. New Phytol. **142:**531–538.
13. **Bode, G., F. Mauch, H. Ditschuneit, and P. Malfertheiner.** 1993. Identification of structures containing polyphosphate in *Helicobacter pylori*. J. Gen. Microbiol. **139:**3029–3033.
14. **Bolesch, D. G., and J. D. Keasling.** 2000. The effect of monovalent ions on polyphosphate binding to *Escherichia coli* exopolyphosphatase. Biochem. Biophys. Res. Commun. **274:**236–241.
15. **Bolesch, D. G., and J. D. Keasling.** 2000. Polyphosphate binding and chain length recognition of *Escherichia coli* exopolyphosphatase. J. Biol. Chem. **275:**33814–33819.
16. **Bücking, H., S. Beckmann, W. Heyser, and I. Kottke.** 1998. Elemental contents in vacuolar granules of ectomycorrhizal fungi measured by EELS and EDXS. A comparison of different methods and preparation techniques. Micron **29:**53–61.
17. **Bücking, H., and W. Heyser.** 1999. Elemental composition and function of polyphosphates in ectomycorrhizal fungi—an X-ray microanalytical study. Mycol. Res. **103:**31–39.
18. **Castuma, C. E., R. Huang, A. Kornberg, and R. N. Reusch.** 1995. Inorganic polyphosphates in the acquisition of competence in *Escherichia coli*. J. Biol. Chem. **270:**12980–12983.
19. **Clark, J. E., and H. G. Wood.** 1987. Preparation of standards and determination of sizes of long-chain polyphosphates by gel electrophoresis. Anal. Biochem. **161:**280–290.
20. **Cole, L., D. A. Orlovich, and A. E. Ashford.** 1998. Structure, function, and motility of vacuoles in filamentous fungi. Fungal Genet. Biol. **24:**86–100.
21. **Jacobson, L., M. Halmann, and J. Yariv.** 1982. The molecular composition of the volutin granule of yeast. Biochem. J. **201:**473–479.
22. **Jäger, K. M., C. Johansson, U. Kunz, and H. Lehmann.** 1997. Sub-cellular element analysis of a cyanobacterium (*Nostoc* sp.) in symbiosis with *Gunnera manicata* by ESI and EELS. Bot. Acta **110:**151–157.
23. **Kaffman, A., I. Herskowitz, R. Tjian, and E. K. O'Shea.** 1994. Phosphorylation of the transcription factor PHO4 by a cyclin-CDK complex, PHO80-PHO85. Science **263:**1153–1156.
24. **Kim, K.-S., N. N. Rao, C. D. Fraley, and A. Kornberg.** 2002. Inorganic polyphosphate is essential for long-term survival and virulence factors in *Shigella* and *Salmonella* spp. Proc. Natl. Acad. Sci. USA **99:**7675–7680.
25. **Kornberg, A., N. N. Rao, and D. Ault-Riché.** 1999. Inorganic polyphosphate: a molecule of many functions. Annu. Rev. Biochem. **68:**89–125.
26. **Kulaev, I. S., V. M. Vagabov, and T. V. Kulakovskaya.** 2004. Localization of polyphosphates in cells of prokaryotes and eukaryotes, p. 53–63. *In* I. S. Kulaev, V. M. Vagabov, and T. V. Kulakovskaya (ed.), The biochemistry of inorganic polyphosphates, 2nd ed. John Wiley & Sons, West Sussex, United Kingdom.
27. **Kumble, K. D., and A. Kornberg.** 1995. Inorganic polyphosphate in mammalian cells and tissues. J. Biol. Chem. **270:**5818–5822.
28. **Kuroda, A., K. Nomura, R. Ohtomo, J. Kato, T. Ikeda, N. Takiguchi, H. Ohtake, and A. Kornberg.** 2001. Role of inorganic polyphosphate in promoting ribosomal protein degradation by the Lon protease in *E. coli*. Science **293:**705–708.
29. **Kuroda, A., S. Tanaka, T. Ikeda, J. Kato, N. Takiguchi, and H. Ohtake.** 1999. Inorganic polyphosphate kinase is required to stimulate protein degradation and for adaptation to amino acid starvation in *Escherichia coli*. Proc. Natl. Acad. Sci. USA **96:**14264–14269.
30. **Marchesini, N., F. A. Ruiz, M. Vieira, and R. Docampo.** 2002. Acidocalci-

somes are functionally linked to the contractile vacuole of *Dictyostelium discoideum*. J. Biol. Chem. **277:**8146–8153.
31. **Motulsky, H., and A. Christopoulos.** 2003. Fitting models to biological data using linear and nonlinear regression. A practical guide to curve fitting. GraphPad Software, San Diego, Calif.
32. **Ogawa, N., J. DeRisi, and P. O. Brown.** 2000. New components of a system for phosphate accumulation and polyphosphate metabolism in *Saccharomyces cerevisiae* revealed by genomic expression analysis. Mol. Biol. Cell **11:** 4309–4321.
33. **Orlovich, D. A., and A. E. Ashford.** 1993. Polyphosphate granules are an artefact of specimen preparation in the ectomycorrhizal fungus *Pisolithus tinctorius*. Protoplasma **173:**91–102.
34. **Pestov, N. A., T. V. Kulakovskaya, and I. S. Kulaev.** 2004. Inorganic polyphosphate in mitochondria of *Saccharomyces cerevisiae* at phosphate limitation and phosphate excess. FEMS Yeast Res. **4:**643–648.
35. **Rao, N. N., S. Liu, and A. Kornberg.** 1998. Inorganic polyphosphate in *Escherichia coli*: the phosphate regulon and the stringent response. J. Bacteriol. **180:**2186–2193.
36. **Rashid, M. H., and A. Kornberg.** 2000. Inorganic polyphosphate is needed for swimming, swarming, and twitching motilities of *Pseudomonas aeruginosa*. Proc. Natl. Acad. Sci. USA **97:**4885–4890.
37. **Rashid, M. H., N. N. Rao, and A. Kornberg.** 2000. Inorganic polyphosphate is required for motility of bacterial pathogens. J. Bacteriol. **182:**225–227.
38. **Rees, G. N., G. Vasiliadis, J. W. May, and R. C. Bayly.** 1992. Differentiation of polyphosphate and poly-beta-hydroxybutyrate granules in an *Acinetobacter* sp. isolated from activated sludge. FEMS Microbiol. Lett. **73:**171–173.
39. **Rodrigues, C. O., F. A. Ruiz, P. Rohloff, D. A. Scott, and S. N. J. Moreno.** 2002. Characterization of isolated acidocalcisomes from *Toxoplasma gondii* tachyzoites reveals a novel pool of hydrolyzable polyphosphate. J. Biol. Chem. **277:**48650–48656.
40. **Rubin, G. M.** 1973. The nucleotide sequence of *Saccharomyces cerevisiae* 5.8 S ribosomal ribonucleic acid. J. Biol. Chem. **248:**3860–3875.
41. **Ruiz, F. A., N. Marchesini, M. Seufferheld, Govindjee, and R. Docampo.** 2001. The polyphosphate bodies of *Chlamydomonas reinhardtii* possess a proton-pumping pyrophosphatase and are similar to acidocalcisomes. J. Biol. Chem. **276:**46196–46203.
42. **Ruiz, F. A., C. O. Rodrigues, and R. Docampo.** 2001. Rapid changes in polyphosphate content within acidocalcisomes in response to cell growth, differentiation, and environmental stress in *Trypanosoma cruzi*. J. Biol. Chem. **276:**26114–26121.
43. **Schröder, H. C., B. Lorenz, L. Kurz, and W. E. G. Müller.** 1999. Inorganic polyphosphate in eukaryotes: enzymes, metabolism and function, p. 45–81. *In* H. C. Schröder and W. E. G. Müller (ed.), Prog. Mol. Subcell. Biol., vol. 23. Springer-Verlag, Berlin, Germany.
44. **Serafim, L. S., P. C. Lemos, C. Levantesi, V. Tandoi, H. Santos, and M. A. M. Reis.** 2002. Methods for detection and visualization of intracellular polymers stored by polyphosphate-accumulating microorganisms. J. Microbiol. Methods **51:**1–18.
45. **Shiba, T., D. Nishimura, Y. Kawazoe, Y. Onodera, K. Tsutsumi, R. Nakamura, and M. Ohshiro.** 2003. Modulation of mitogenic activity of fibroblast growth factors by inorganic polyphosphate. J. Biol. Chem. **278:**26788–26792.
46. **Shiba, T., K. Tsutsumi, H. Yano, Y. Ihara, A. Kameda, K. Tanaka, H. Takahashi, M. Munekata, N. N. Rao, and A. Kornberg.** 1997. Inorganic polyphosphate and the induction of *rpoS* expression. Proc. Natl. Acad. Sci. USA **94:**11210–11215.
47. **Suresh, N., R. Warburg, M. Timmerman, J. Wells, M. Coccia, M. F. Roberts, and H. O. Halvorson.** 1985. New strategies for the isolation of microorganisms responsible for phosphate accumulation. Water Sci. Technol. **17:**99–111.
48. **Tijssen, J. P. F., H. W. Beekes, and J. van Steveninck.** 1982. Localization of polyphosphates in *Saccharomyces fragilis*, as revealed by 4′,6-diamidino-2-phenylindole fluorescence. Biochim. Biophys. Acta **721:**394–398.
49. **Tijssen, J. P. F., T. M. A. R. Dubbelman, and J. van Steveninck.** 1983. Isolation and characterization of polyphosphates from the yeast cell surface. Biochim. Biophys. Acta **760:**143–148.
50. **Tijssen, J. P. F., and J. van Steveninck.** 1984. Detection of a yeast polyphosphate fraction localized outside the plasma membrane by the method of phosphorus-31 nuclear magnetic resonance. Biochem. Biophys. Res. Commun. **119:**447–451.
51. **Trilisenko, L. V., V. M. Vagobov, and I. S. Kulaev.** 2002. The content and chain length of polyphosphates from vacuoles of *Saccharomyces cerevisiae* VKM Y-1173. Biochemistry (Moscow) **67:**711–716.
52. **Turnau, K., I. Kottke, and F. Oberwinkler.** 1993. *Paxillus involutus Pinus sylvestris* mycorrhizae from heavily polluted forest. I. Elemental localization using electron energy loss spectroscopy and imaging. Bot. Acta **106:**213–219.
53. **Urech, K., M. Dürr, T. Boller, and A. Wiemken.** 1978. Localization of polyphosphate in vacuoles of *Saccharomyces cerevisiae*. Arch. Microbiol. **116:**275–278.
54. **Vořišek, J., A. Knotková, and A. Kotyk.** 1982. Fine cytochemical localization of polyphosphates in the yeast *Saccharomyces cerevisiae*. Zbl. Mikrobiol. **137:**421–432.
55. **Wood, H. G., and J. E. Clark.** 1988. Biological aspects of inorganic polyphosphates. Annu. Rev. Biochem. **57:**235–260.
56. **Wurst, H., and A. Kornberg.** 1994. A soluble exopolyphosphatase of *Saccharomyces cerevisiae*. purification and characterization. J. Biol. Chem. **269:** 10996–11001.
57. **Wurst, H., T. Shiba, and A. Kornberg.** 1995. The gene for a major exopolyphosphatase of *Saccharomyces cerevisiae*. J. Bacteriol. **177:**898–906.